[1]Mihir B. Chaudhari
[2]Nirav D. Patel
[3]Priyank R. Bhavsar
[4]Ashok L. Vaghamshi
[5]Sanjay D. Mali
[6]Vinod N. Patni
[7]Pritesh K. Jaradi
[8]Tapan Trivedi
[9]Chanrakishor Gupta

Implementation of Shunt Active Power Filter Using DSP Controller Based on Synchronous Reference Frame for Harmonic Mitigation

Journal of Electrical Systems

Abstract: - This research paper introduces the concept of a shunt active power filter (SAPF) that leverages synchronous-reference-frame (SRF) theory to mitigate harmonics in the power system. The SAPF works by injecting a compensating current at the point of common coupling (PCC) to counteract the harmonics in the line and restore sinusoidal current waveforms. It employs a three-phase current-controlled voltage source inverter (VSI) with a DC link capacitor for active filtering. An SRF algorithm is designed for a low-voltage laboratory prototype utilizing the TMS320F28335 Digital Signal Processor (DSP). The experimental findings affirm that the control strategy effectively aligns with the recommended harmonic standard limits of IEEE 519-1992.

Keywords: Active Power Filter, DSP controller, Synchronous Reference Frame

I. INTRODUCTION

In electrical power systems, the prevalence of harmonic current distortion presents a significant challenge. This distortion arises from the widespread use of non-linear loads, such as diode or thyristor-based converters, as well as various large load-utilizing devices and appliances. While passive filters are commonly used, they have limitations, including being less adaptable, load-dependent, and inflexible [1]. Shunt active power filters (SAPFs) have been developed to address these issues, mitigating current harmonic distortions and improving power factors. Depending on the requirements at the Point of Common Coupling (PCC), shunt active power filters can serve various purposes, including power factor correction, voltage regulation, load balancing, voltage flicker reduction, or a combination of these [1, 2]. Figure 1 illustrates the fundamental compensation principle of the SAPF: it identifies harmonic and reactive power generated from the load and provides a compensating current into the system to neutralize the existing harmonics in the load. In the traditional p-q theory-based control approach for SAPFs [3], the compensation current references are generated based on the measurement of load currents. Most methods utilize instantaneous p-q theory and compute currents in stationary reference frames.

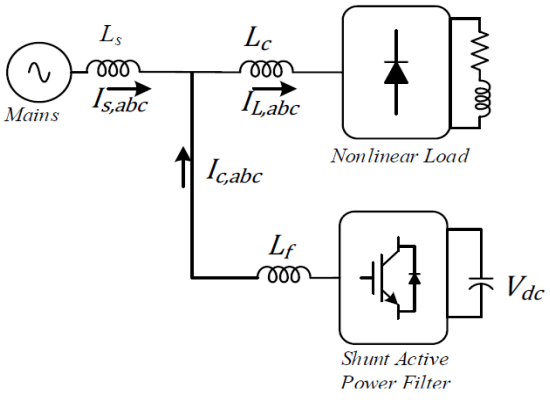

Fig. 1. Basic block diagram of SAPF

[1] Electrical Engineering Department, GEC, Gandhinagar, mihirchaudhari@gecg28.ac.in
[2] Electrical Engineering Department, GEC, Gandhinagar, niravdpatel@gecg28.ac.in
[3] Electrical Engineering Department, GEC, Gandhinagar, ashokvaghamshi@gecg28.ac.in
[4] Electrical Engineering Department, GEC, Gandhinagar, prbhavsar@gecg28.ac.in
[5] Mechanical Engineering Department, GEC, Gandhinagar, malisanjay28@gmail.com
[6] Mechanical Engineering Department, GEC, Gandhinagar, patnivinod78@gmail.com
[7] Mechanical Engineering Department,, GEC, Bhuj, jaradi.007@gmail.com
[8] Electrical Engineering Department, Marwadi Education Foundation, tapankumar.trivedi@marwadieducation.edu.in
[9] Institute of Plasma Research, Bhat, ckgupta@ipr.res.in

The researchers cited in reference [4] illustrated the use of FPGA for developing an algorithm based on Synchronous Reference Frame (SRF) theory. With the assistance of advancements in high-performance DSP, as discussed in reference [5], the realization of instantaneous algorithms [6, 7, 8] has become viable. This study focuses on the creation of an algorithm and the evaluation of the performance of shunt active power filters in the synchronous reference frame. The approach involves decomposing currents to generate instantaneous active and reactive powers, computing components for fundamental current generation, and producing reference currents using a two-kVA laboratory prototype.

II. SYNCHRONOUS REFERENCE FRAME THEORY

Referencing the current generation described here is based on time domain development. The synchronous reference frame (SRF) theory is widely utilised due to its simplicity and reliance on algebraic calculations. In this approach, the three-phase load current (i_{La}, i_{Lb}, i_{Lc}) is transformed into two instantaneous components - active (i_{Ld}) and reactive (i_{Lq}) - within a rotating synchronous frame aligned with the positive sequence of the system voltage. The SRF method utilises direct (d-q) and inverse (d-q) park transformations, enabling the evaluation of specific harmonic components of the input signals. The reference frame transformation involves converting a stationary three-phase a-b-c reference frame system to a synchronous reference frame dq0, where the two-phase direct axis (d) and quadrature axis (q) components rotate at the synchronous speed ω_e. This speed, ω_e, represents the angular electrical speed of the rotating magnetic field of the three-phase supply, given by $\omega_e = 2\pi f$. If θ is the transformation angle, then the current transformation from ABC to dq0 frame is calculated using the following formulas:

$$[i_{dq0}]=[T][i_{abcs}] \quad (1)$$

Where

$$the\ T = \sqrt{\frac{2}{3}}\begin{bmatrix} cos\theta & \cos(\theta-\frac{2\pi}{3}) & \cos(\theta+\frac{2\pi}{3}) \\ sin\theta & sin(\theta-\frac{2\pi}{3}) & sin(\theta+\frac{2\pi}{3}) \\ \frac{1}{\sqrt{2}} & \frac{1}{\sqrt{2}} & \frac{1}{\sqrt{2}} \end{bmatrix}$$

And

$$\theta = \int \omega_e dt + \theta_0$$

Similarly, voltage equations can be derived for all phases. The instantaneous active and reactive power from a set of two-phase voltages and currents is given by

$$p_L = \frac{3}{2}(v_d i_{Ld} + v_q i_{Lq})$$
$$q_L = \frac{3}{2}(v_q i_{Lq} - v_d i_{Lq}) \quad (2)$$

Whenever the synchronous frame is aligned to the a-phase axis, the quadrature axis component is reduced to zero, i.e. vq = 0. Therefore, the power equations are reduced to:

$$p_L = \frac{3}{2} v_d i_{Ld}$$
$$q_L = -\frac{3}{2} v_d i_{Lq} \quad (3)$$

The equations above demonstrate that it is possible to independently control active and reactive power by regulating the current along the d q axis (id and iq). In the case of a non-linear load, the current can be separated into a DC component and oscillating components, which are responsible for the fundamental and harmonic currents, respectively.

$$i_{Ldq} = \overline{i_{Ldq}} + \widetilde{i_{Ldq}} \quad (4)$$

The DC component of current in the d-axis is primarily responsible for the average active power transfer between the source and the load. An inverse park transformation is carried out to obtain the fundamental in-phase component of the current. Due to switching losses, the component of current that fulfils the charging requirement of the capacitor should also be taken into account

$$\begin{bmatrix} i_{sa}^* \\ i_{sb}^* \\ i_{sc}^* \end{bmatrix} = [T]^{-1} \begin{bmatrix} \overline{-i_{Ld}} + i_{loss} \\ 0 \\ 0 \end{bmatrix} \quad (5)$$

The compensating current reference can be determined by subtracting the load current from the fundamental reference source current

$$\begin{bmatrix} i_{ca}^* \\ i_{cb}^* \\ i_{cc}^* \end{bmatrix} = \begin{bmatrix} i_{sa}^* \\ i_{sb}^* \\ i_{sc}^* \end{bmatrix} - \begin{bmatrix} i_{La}^* \\ i_{Lb}^* \\ i_{Lc}^* \end{bmatrix} \quad (6)$$

A hysteresis controller determines the switching equation based on equation (7), where switching action occurs based on the band of current error values.

$$S_i(k+1) = \begin{cases} 0 & \Delta i < -\frac{Hb}{2} \\ S_i(k) & \frac{Hb}{2} < \Delta i < -\frac{Hb}{2} \\ 0 & \Delta i > \frac{Hb}{2} \end{cases} \quad (7)$$

III. Implementation of DSP-based Control Algorithm

In Figure 2, you can see the overview of the implementation of the Synchronous Reference Frame theory-based control strategy. With this theory, reference current signals are generated using the controller, and the output references are compared with the actual current in the current minor loop. Generating reference currents involves straightforward transformation equations, while macros such as Phase Locked Loop (PLL), Moving Average Filter (MAF), and current controllers are utilised. In this section, the implementation of these macros is further elaborated.

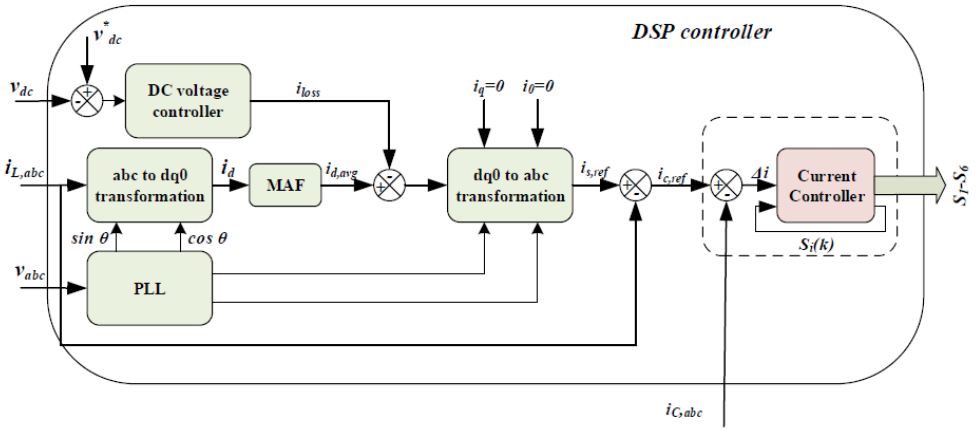

Fig. 2. Block diagram of SRF-based current control strategy

A. *Phase-locked loop*

Using the synchronous reference frame theory, the DSP implements a software-based Phase Locked Loop algorithm to lock the frequency and angle. To explain, we measure three-phase voltages and transform them into a rotating reference frame using Equation (1). As a result, we obtain the d-axis and q-axis components of the voltages.

$$v_d = Vcos(\omega_e t - \theta_{PLL})$$
$$v_q = Vsin(\omega_e t - \theta_{PLL}) \quad (8)$$

If the Phase Locked Loop is adequately synchronised, the q-axis component of the grid voltage reduces to:

$$v_q = V(\omega_e t - \theta_{PLL}) \quad (9)$$

Any error in the measured angle θPLL will be immediately reflected at the output of vq.

$$\omega_{LPF}(k) = \omega_{LPF}(k-1) + v_q(k) \times k_1 + v_q(k-1) \times k_2 \quad (10)$$

Please take note of the following text:

Where k1 and k2 are constants for the low-pass filter provided at the output of vq. The values of these constants are calculated based on the PLL's desired performance and the sampling frequency. For the sample time of 16 µs used in this program, the values of k1 and k2 are 222.3 and -221.6, respectively. The synchronised frequency of the grid is given by:

$$\omega_{grid}(k) = \omega_{init}(k) + \omega_{LPF}(k) \quad (11)$$

B. *Moving Average Filter*

A Moving Average Filter is a Finite Impulse Response filter and is easy to implement, owing to the limited data that a DSP can store. Mathematically, the filter equation is given by

$$\overline{i_d} = \frac{1}{N}\sum_{k-1}^{N} i_d(k) \quad (12)$$

However, executing the above equation may be time-consuming as the data must be read N times from the memory. Hence, a cumulative moving average approach is adopted. This can be expressed as

$$\overline{i_d} = \frac{N\overline{i_d}(k-1)+i_d(k)}{N+1} \quad (13)$$

Instead of generating references using a digital-to-analogue converter and developing a hysteresis current controller, the actual three-phase compensating currents are sensed, allowing for implementing a complex current controller. In this study, a simple hysteresis current controller (HCC) has been developed. However, more complex linear or non-linear current controllers can be targeted in future work. In the case of hysteresis current control, the error vector is input to the current controller. The controller will maintain its previous state, Si(k), as long as no violation of the present condition is detected. The next preferable voltage vector is applied if the current error vector hits or crosses the boundary.

IV. Experimental Results and Discussion

To assess the performance of the SAPF, a prototype SAPF model was created and tested in the lab using TMS320F28335 as the core. Load currents and compensating currents were measured using LEM LA55P Hall Effect current sensors. Three-phase voltages and DC link voltage were also measured using LV20-P voltage sensors. The outputs of the sensors were buffered and conditioned to ensure proper operation of the ADC. Experimental parameters are detailed in Appendix 5.

The three-phase voltages were measured and sent to the ADC, which then executed the Phase Locked Loop algorithm at 16 µs intervals. The component responsible for the fundamental in-phase current was calculated based on the load current values. However, as the SAPF is intended to supply harmonics, the d-q components responsible for current distortion were calculated, as depicted in Figure 4. The three-phase compensating currents were computed using the components responsible for harmonic generation, as shown in Figure 3. It is important to note that the summation of the load current and compensating current resulted in a pure sinusoid. The SAPF performance under steady-state conditions is illustrated in Figure 5.

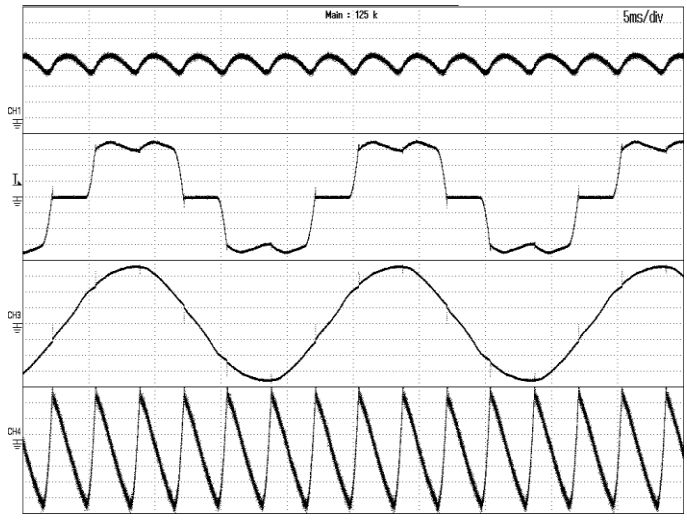

Fig. 3. Generation of dq components of load current using SRF theory (a) Ch-1: direct axis component of load current (b) Ch-2: Actual Load Current of Phase-A (c) Ch-3: Source Phase Voltage V_a (d) Ch-4: quadrature axis component of load current, X-axis: 5 ms/div

The Total Harmonic Distortion (THD) of all three phases before and after compensation was measured using the Fluke 430-II Power Quality Analyzer. Before compensation, the THD for all phases was 28.6%, which was reduced to 2.1% after compensation. Notably, the achieved THD is well below the IEEE 519-1992 standard.

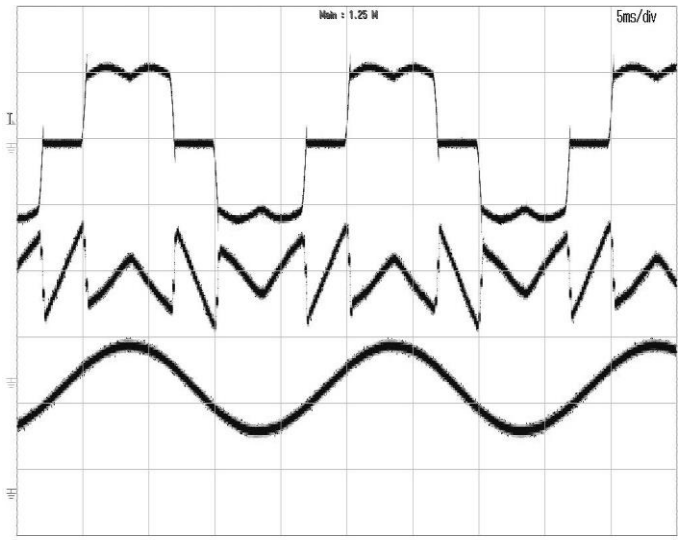

Fig. 4. Actual load current, reference compensating current and fundamental source current: Ch-1: Actual load current (2A/div), Ch-2: Reference Compensating current (1A/div), Ch-3: Reference source current (2A/div), X-axis: 5 ms/div

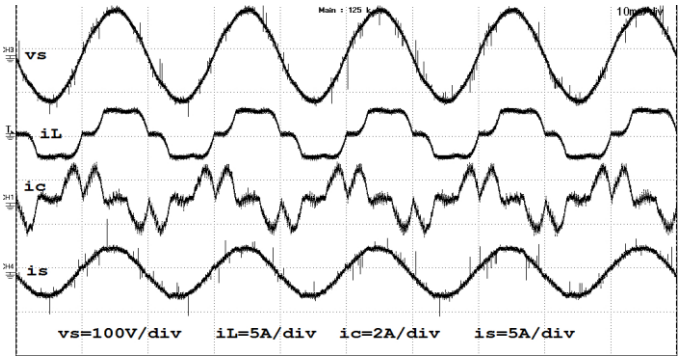

Fig.5 Basic block diagram of SAPF Steady-state performance of Shunt Active Power Filter (a) Ch-1: Source Phase Voltage Va (100V/div) (b) Ch-2: Load CurrentiL(5A/div) (c) Ch-3: Compensating Current ic(2A/div) (c) Ch-4: Source Current is (5A/div), X-axis: (5 ms/div)

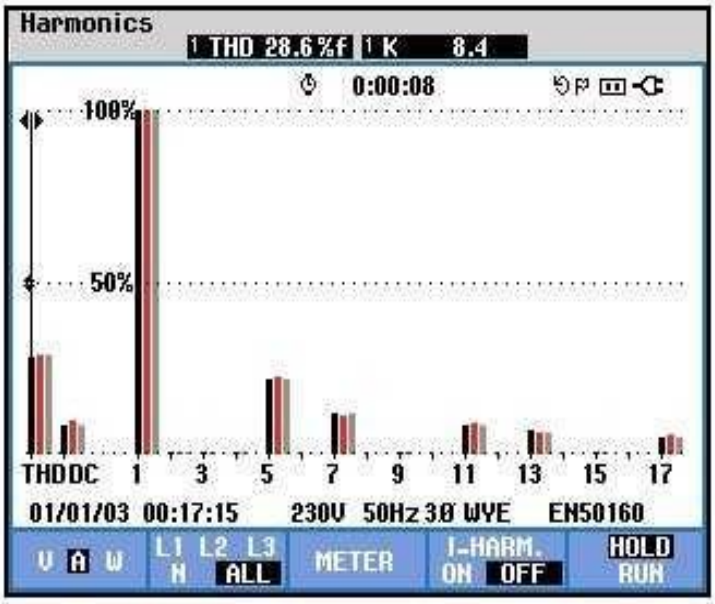

Fig. 6. FFT Spectrum and THD of Three-phase Line Current-Before Compensation

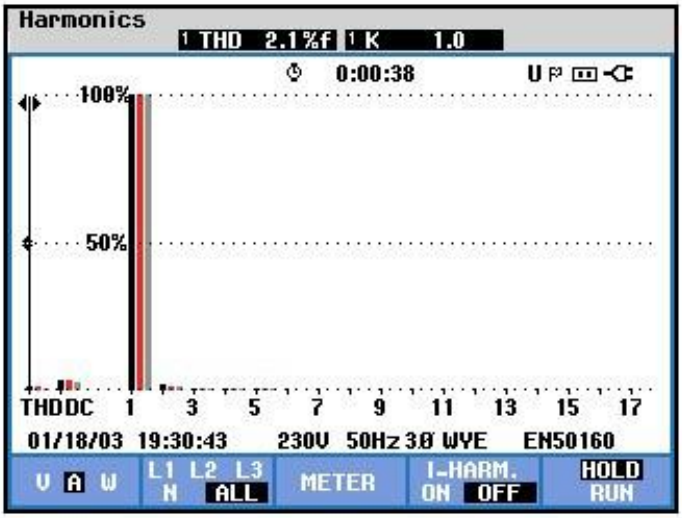

Fig.7 FFT Spectrum and THD of Three-phase Line Current-after compensation

V. CONCLUSIONS

The paper explores a control method based on SRF theory for the SAPF. Experimental tests have been conducted to validate the control algorithms' effectiveness. The experimental test results, using TMS320F28335 DSP, showcase the performance of the control algorithm for the SAPF. Both simulations and experimental results affirm that the control algorithm for SAPF is straightforward and easily implementable. The paper presents experimental results obtained from a laboratory model and theoretical analysis to confirm the viability and effectiveness of the control method under non-linear load conditions.

REFERENCES

[1] H. Akagi, Instantaneous power theory and application to power conditioning, John Wiley & Sons, 2004.

[2] K. A. H. Bhim Singh, A. Chandra, A review of active filters for power quality improvement, IEEE Transactions On Industrial Electronics 46 (1999) 960–971.

[3] K. R. Chaudhari, T. A. Trivedi, Analysis on the control strategy of shunt active power filter for the three-phase three-wire system, in Transmission Distribution Conference and Exposition - Latin America (PES T D-LA), 2014 IEEE PES, 2014, pp. 1–6. doi:10.1109/TDC-LA.2014.6955179.

[4] Z. Shu, Y. Guo, J. Lian, Steady-state and dynamic study of active power filter with efficient fpga-based control algorithm, IEEE Transactions on Industrial Electronics 55 (4) (2008) 1527–1536. doi:10.1109/TIE.2008.917151.

[5] T. Instruments, Datasheet on TMS320F28335, Texas Instruments, f Edition (2007).

[6] I. Axente, A 12-kva dsp-controlled laboratory prototype upqc capable of mitigating unbalance in source voltage and load current, IEEE Transactions on Power Electronics 25 (2010) 1471–1479.

[7] S. Rahmani, A. Hamadi, N. Mendalek, K. Al-Haddad, A new control technique for three-phase shunt hybrid power filter, IEEE Transactions on Industrial Electronics 56 (8) (2009) 2904–2915. doi:10.1109/TIE.2008.2010829.

[8] G. J. Bruce S. Chen, Direct power control of active filters with averaged switching frequency regulation, IEEE Transaction on Power Electronics 23 (2008) 2729–2737.